ACS APPLIED MATERIALS & INTERFACES

Letter

www.acsami.org

GHz Properties of Magnetophoretically Aligned Iron-Oxide Nanoparticle Doped Polymers

Ferruccio Pisanello,*[,†,‡] Rosa De Paolis,[§] Daniela Lorenzo,[†] Pablo Guardia,[⊥] Simone Nitti,[⊥] Giuseppina Monti,[§] Despina Fragouli,[⊥] Athanassia Athanassiou,[⊥] Luciano Tarricone,[§] Liberato Manna,[⊥] Massimo De Vittorio,[†,§,#] and Luigi Martiradonna[†]

[†]Center for Biomolecular Nanotechnologies@UniLe, Istituto Italiano di Tecnologia, 73010 Arnesano (LE), Italy

[‡]Center for Neuroscience and Cognitive Systems@UniTn, Istituto Italiano di Tecnologia, 38068 Rovereto (TN), Italy

[§]Dip. di Ingegneria dell'Innovazione, Università del Salento, Via Arnesano, 73100 Lecce - Italy

[⊥]Nanophysics and Nanochemistry Departments, Istituto Italiano di Tecnologia, via Morego 30, 16163 Genova, Italy

[#]National Nanotechnology Laboratory, Istituto Nanoscienze-CNR, Via Arnesano, 73100 Lecce, Italy

Supporting Information

ABSTRACT: We show that assembled domains of magnetic iron-oxide nanoparticles (IONPs) are effective at increasing the dielectric permittivity of polydimethylsiloxane (PDMS) nanocomposites in the GHz frequency range. The assembly has been achieved by means of magnetophoretic transport and its efficacy, as well as the electromagnetic properties of the nanocomposite, has been found to depend on IONPs diameter. Remarkably, the dielectric permittivity increase has been obtained by keeping dielectric and magnetic losses very low, making us envision the suitability of nanocomposites based on aligned IONPs as substrates for radiofrequency applications.

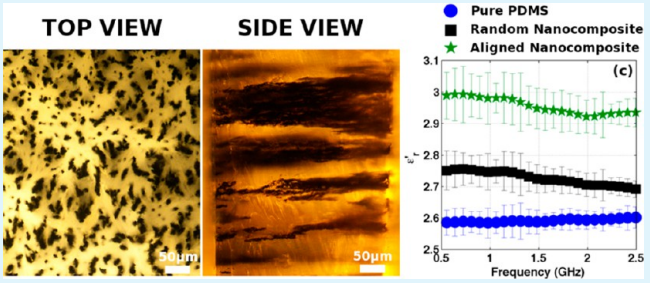

KEYWORDS: *nanocomposite, polydimethylsiloxane, magnetic nanoparticles, magnetophoresis, radiofrequency*

INTRODUCTION

Polymer nanocomposites (PNCs) consist of a polymeric matrix filled with nanomaterials that can be able to enhance or induce peculiar properties at the macroscale level.[1] The possibility to improve mechanical, electrical, and optical performances of pure polymers has risen the attention of the scientific community toward these materials, and several important results have been achieved in recent years.[2−8] In particular, PNCs with tunable dielectric and magnetic properties are a promising toolbox for the development of devices operating in the radiofrequency (RF) range. Indeed, polymer matrices have the great advantages of mechanical flexibility, lightweight and ease of manipulation; their doping with nanoparticles (NPs) has been demonstrated to be an effective method to modify their electrical permittivity (ε_r) and magnetic permeability (μ_r), allowing the modulation of their electromagnetic response.[9−14] Both ε_r and μ_r are complex quantities ($\varepsilon_r = \varepsilon'_r - j\varepsilon''_r$ and $\mu_r = \mu'_r - j\mu''_r$) and are related to materials response under an electromagnetic stimulus. For instance, substrates for RF circuits with high ε'_r and/or μ'_r allow to decrease the size of devices and radiative elements and to obtain high power efficiency through the minimization of both dielectric and magnetic loss tangents, defined as $\tan\delta_\varepsilon = \varepsilon''_r/\varepsilon'_r$ and $\tan\delta_\mu = \mu''_r/\mu'_r$, respectively.[15] ε_r and μ_r values in soft materials are also engineered to optimize the performance of electromagnetic wave absorbers or radiofrequency shields.[16−18]

Promising filler materials to achieve these goals are represented by ferromagnetic and superparamagnetic NPs, namely iron-oxide NPs (IONPs),[11,13,19−21] $NiZnFe_2O_4$ NPs,[22] core/shell Fe/SiO_2 NPs[23] or Fe/ZnO NPs,[24] Co_xNi_{1-x} NPs,[11] and SnO_2 NPs.[25] The peculiarity of these materials is that magneto-dielectric properties of the realized PNC depend on NPs intrinsic properties: doping of polymers with superparamagnetic NPs does not affect polymers' μ_r and induces an increase of ε_r,[19] whereas doping with ferromagnetic NPs acts on both ε_r and μ_r.[19] Moreover, the net magnetic moment arising from the NPs can be exploited to obtain ordered NP assemblies,[26−30] thus inducing also an anisotropic response of the PNC.[28,31,32] For instance, exposure of IONPs dispersed in a polymeric host matrix to an external magnetic field during solvent evaporation and/or polymer curing enables the realization of anisotropic magnetic films, due to the magnetophoretic transport and assembly of the IONPs parallel to the field direction, resulting in wirelike structures.[28−30] Therefore,

Received: January 18, 2013
Accepted: March 28, 2013
Published: March 28, 2013

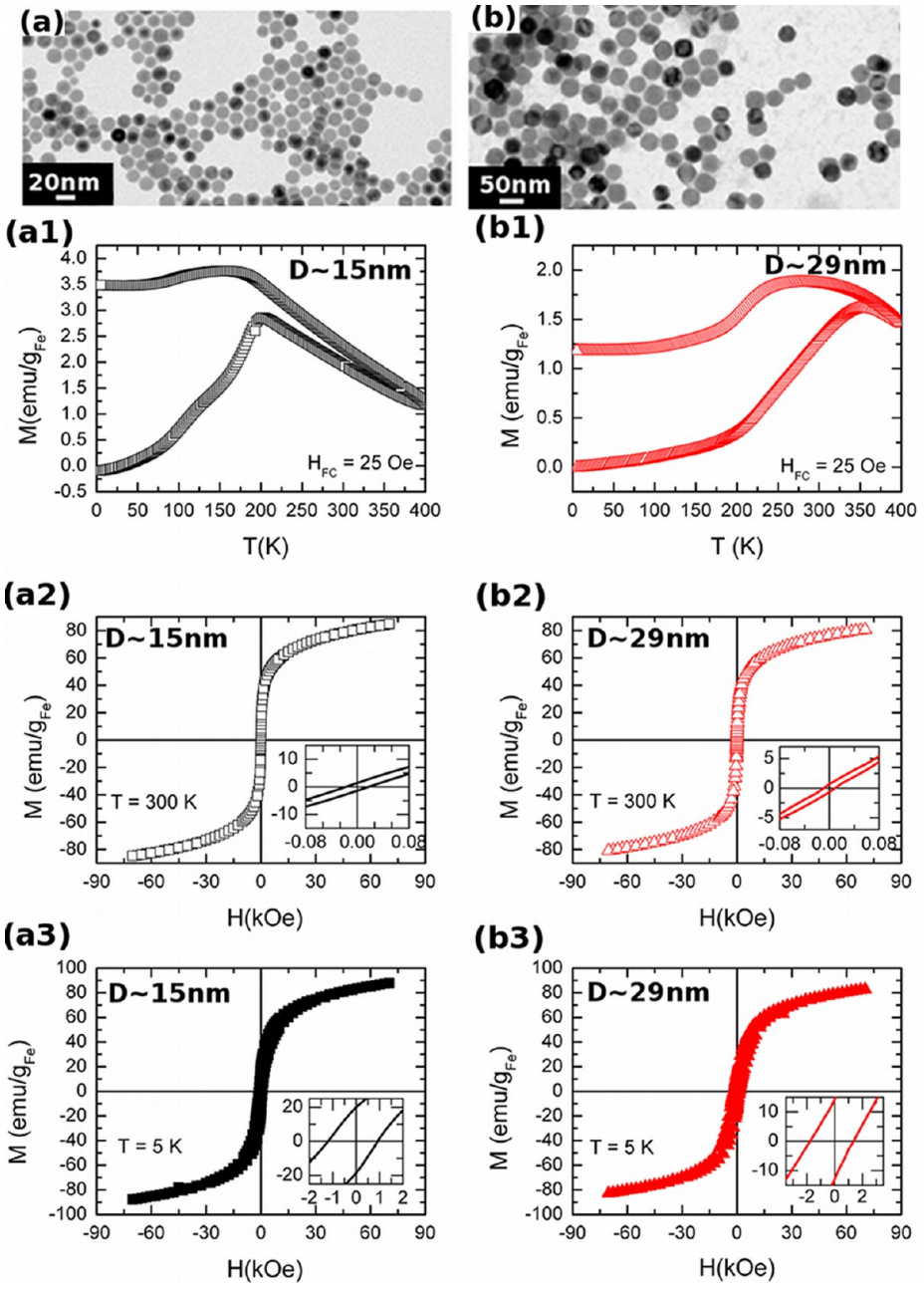

Figure 1. Iron-oxide NPs characterization. (a, b) Transmission electron microscope micrographs of iron-oxide NPs of diameter (a) $D \approx 15$ nm and (b) $D \approx 29$ nm. (a1, b1) Zero-field-cooled and field-cooled magnetization of IONPs with $D \approx 15$ and $D \approx 29$, respectively. Blocking temperature is T_B~202 ± 2 K for $D \approx 15$ nm and $T_B \approx 356 \pm 2$ K for $D \approx 29$ nm. (a2, b2) Magnetization curves at 300 K for $D \approx 15$ nm and $D \approx 29$ nm, respectively. (a3, b3) Magnetization curves at 5 K for $D \approx 15$ nm and $D \approx 29$ nm, respectively.

nanocomposite films of hundreds of micrometers up to several millimeters size in all directions containing aligned magnetic arrays can be obtained with ordinary laboratory equipment. Both size and shape of these NP assemblies depend on the original particles size, on the type of polymeric matrix and on the magnetic field intensity,[28−30] and one can envision that magneto-dielectric properties of the so-realized PNC depend not just on the magnetic nature of the used NPs,[33] but also on their assembly.

Here we report the RF properties in the GHz frequency range of PNCs based on a polydimethylsiloxane (PDMS) matrix doped with magnetically assembled arrays of colloidal IONPs. PDMS has been chosen as host material by virtue of its low dielectric and magnetic loss tangents, its compatibility with flexible electronics even in presence of NPs and its suitability as a support for pliable, conformal and stretchable RF devices.[21,34−37] The magnetic behavior of the IONPs allows the generation of ordered domains through exposition to static magnetic fields, with the assembly being more effective for bigger IONPs. Remarkably, the aligned IONPs regions are found to have an important role in increasing the PNC dielectric permittivity compared to pure polymer and to polymeric films containing randomly dispersed IONPs. Average tangent loss of all analyzed samples has been found to be lower than ~0.02 up to 2.5 GHz, thus letting us envision the exploitability of the proposed material in low-loss radio-frequency applications.

dx.doi.org/10.1021/am400239b | ACS Appl. Mater. Interfaces 2013, 5, 2908−2914

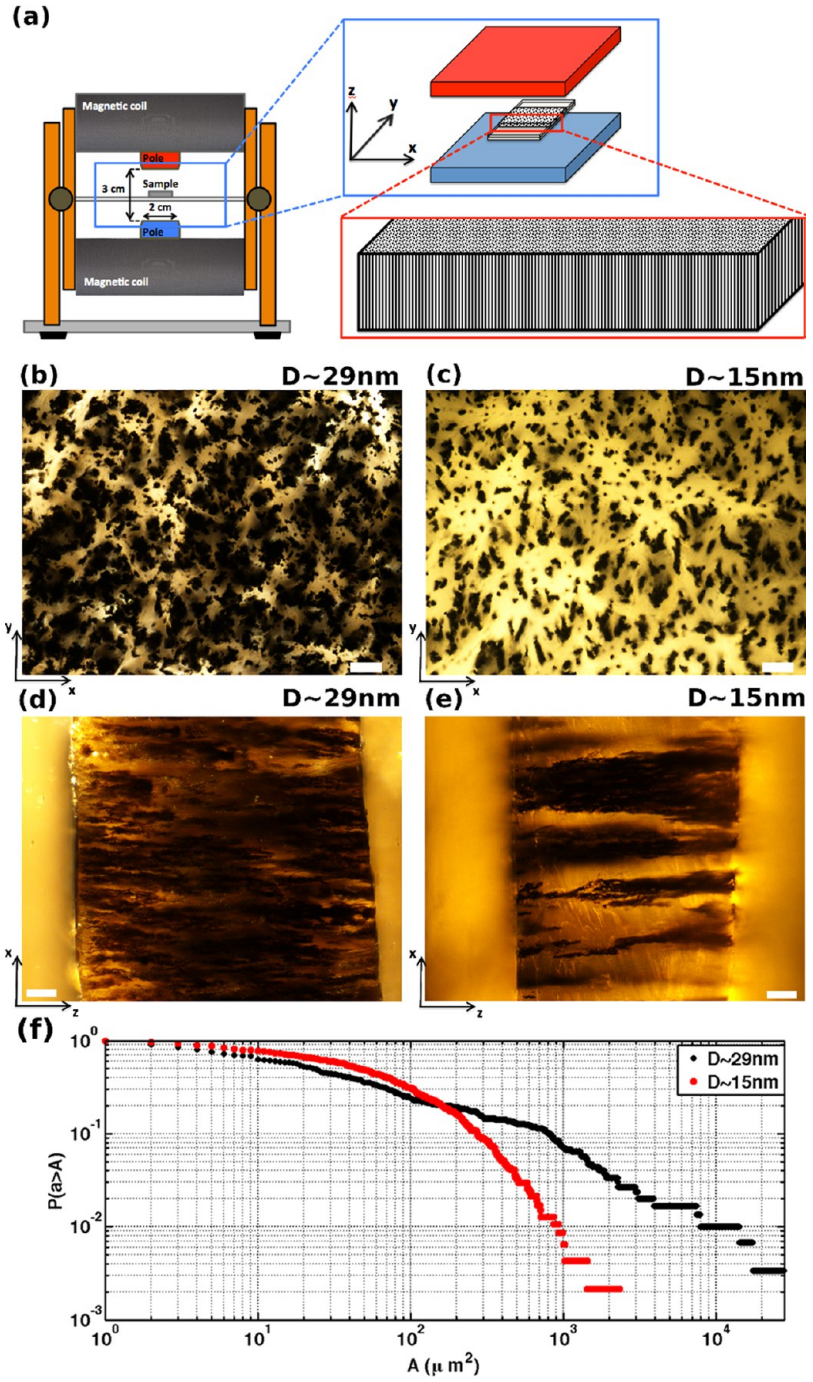

Figure 2. IONPs alignment into the PDMS host matrix. (a) Sketch of the experimental setup used to align NPs during PDMS curing. (b, c) Top view of aligned NPs samples for NPs diameters of $D \approx 29$ nm and $D \approx 15$ nm, respectively. Scale bars are 50 μm. (d, e) Cross-section of the samples parallel to the aligned IONPs domains for IONPs diameters of $D \approx 29$ nm and $D \approx 15$ nm, respectively. Scale bars are 50 μm. (f) Probability to have a cluster area a in the $x-y$ plane bigger than a given value A for NPs diameters of $D \approx 15$ nm (red dots) and $D \approx 29$ nm (black dots).

EXPERIMENTAL PROCEDURE

To prepare IONPs/PDMS nanocomposites, spherical colloidal NPs of two different sizes (diameters $D = 15 \pm 1$ nm and $D = 29 \pm 2$ nm) were dispersed in PDMS prepolymer (from now on we will refer to these two diameters as $D \approx 15$ nm and $D \approx 29$ nm). The monodispersed IONPs were synthesized by a modified surfactant-assisted nonaqueous synthetic approach.[38] Briefly, to synthesize IONPs with $D \approx 15$ nm, 2 mmol of iron(III) oxide hydrated (catalyst grade 30−50 mesh) and 8.5 mmol of Oleic acid (90%) were mixed in 5 g of 1-Octedecene (90%). After degassing at room temperature (RT) for 30 min, the solution was heated up to reflux temperature (320 °C) and kept at this temperature for 1 h under a nitrogen flow. After cooling down, particles were washed by adding 10 mL of 2-propanol followed by centrifugation at 400 rpm for 15 min. A slight increase in oleic acid concentration resulted in the synthesis of IONPs with the higher diameter. The final product was dispersed in toluene (0.316 and 0.238 M of iron atoms in toluene solution for $D \approx 15$ nm and $D \approx 29$ nm, respectively). Transmission electron microcopy (TEM) images of the as-synthesized IONPs are displayed in images a and b in Figure 1

dx.doi.org/10.1021/am400239b | ACS Appl. Mater. Interfaces 2013, 5, 2908−2914

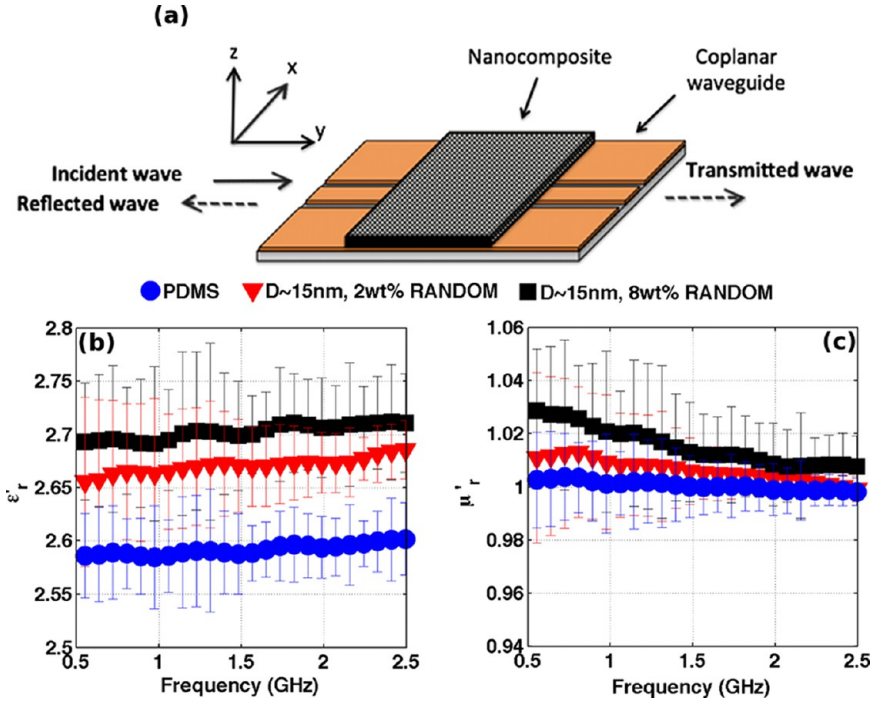

Figure 3. Radiofrequency characterization of random iron-oxide/PDMS PNCs. (a) Sketch of the experimental setup used to measure dielectric permittivity and magnetic permeability of the nanocomposites. (b) Dielectric permittivity and (c) magnetic permeability obtained between 0.5 GHz and 2.5 GHz for pure PDMS (blue dots) and iron-oxide/PDMS PNCs with NPs concentrations of ∼2 wt % (red triangles) and ∼8 wt % (black squares).

(see the Supporting Information for details on IONPs synthesis).

Magnetic properties of IONPs were measured in a commercial SQUID magnetometer Quantum Design MPMSXL (for details, see the Supporting Information). As displayed in Figure 1(a1) and 1(b1), the particles show a blocking temperature (T_B) of 202 ± 2 K and 356 ± 2 K for $D \approx 15$ nm and $D \approx 29$ nm, respectively. Because T_B is well-below RT, $D \approx 15$ nm NPs show a clear superparamagnetic behavior. Whereas, for $D \approx 29$ nm, T_B is slightly above RT (T_B = 356 ± 2 K) showing a weak ferromagnetic behavior at RT. Also hysteresis loops at 5 and 300 K (Figure 1(a2), (a3), (b2), and (b3)) show interesting features: at 5K the coercive fields are higher than those expected for Fe_2O_3 or Fe_3O_4 (see Table S1 in the Supporting Information). This trend, previously observed in literature,[38−40] is commonly associated to a mixture of iron oxide phases in the crystal.[37−39] In addition, even if T_B for $D \approx 29$ nm is slightly above RT, the sample shows only a weak ferromagnetic behavior since their coercive fields at this temperature are almost negligible (for a summary of the magnetic properties see Table S1 in the Supporting Information). All in all, we can conclude that $D \approx 15$ nm has a clearly superparamagnetic behavior at RT, whereas $D \approx 29$ nm shows a weak ferromagnetic behavior, close to the superparamagnetic regime.

To improve uniform dispersion of IONPs in polymer matrix, we previously dissolved PDMS prepolymer (Sylgard 184) in toluene (1:1 volume ratio). The two IONPs/toluene solutions were then added to PDMS in 2 and 8 wt % (IONPs to PDMS prepolymer weight ratio), respectively. The solvent in the final solution was evaporated with a nitrogen gas flow and then the cross-linking agent was added in a typical mixing ratio 10:1 (PDMS prepolymer:cross-linker) and mixed. A small amount of the solution was casted on a PDMS rectangular-shape mold and cured in oven at 140 °C for 10 min. In this way, nanocomposite films of 16 × 20 mm^2, and thicknesses varying from 0.2 mm to 1.2 mm were formed.

For the higher concentration (8 wt %), two nanocomposite films for each IONPs diameter were prepared: the first one contained aligned NP domains along the z axis (see Figures 2a and 3a for axis definition) and the other one had homogeneous filler distribution. To prepare the first film, we placed the mold with the solution under an external magnetic field ($\mathbf{B_0}$) generated by two poles, distant 30 mm from each other, of an electromagnet (Laboratorio Elettrofisico Walker LDJ Scientifico) for 24 h at RT, with the sample surface perpendicular to the direction of $\mathbf{B_0}$. The presence of the magnetic field causes the magnetophoretic transport of the randomly dispersed IONPs in the polymer matrix, and their assembly into chain-like structures along the direction of the field, resulting in the formation of vertical IONPs columns with the similar height as the nanocomposite films. In particular, after placing the noncured PNC under the magnetic field, the magnetic moments of isolated particles and of particle clusters preferentially align along $\mathbf{B_0}$ and the developed field gradients[41] exert forces on the surrounding particles, inducing their assembly in a head-to-tail configuration.[30] The strength of the dipolar moment interactions that allow IONPs assembly depends on several parameters: intensity of the field $\mathbf{B_0}$,[30] clusters size[30] and IONPs diameter.[30,29,42] Differences in alignment effectiveness for different particle diameters are thus expected, because of different particle−particle interactions and attractive van der Waals forces.[30] To obtain the best possible alignment for all the particle diameters investigated in this work, the magnetic field intensity was chosen as the maximum possible in our system, i.e., B_0 = 300 mT. The samples remained under the field for 24h at RT, a time sufficient for the PDMS curing. For the second film with

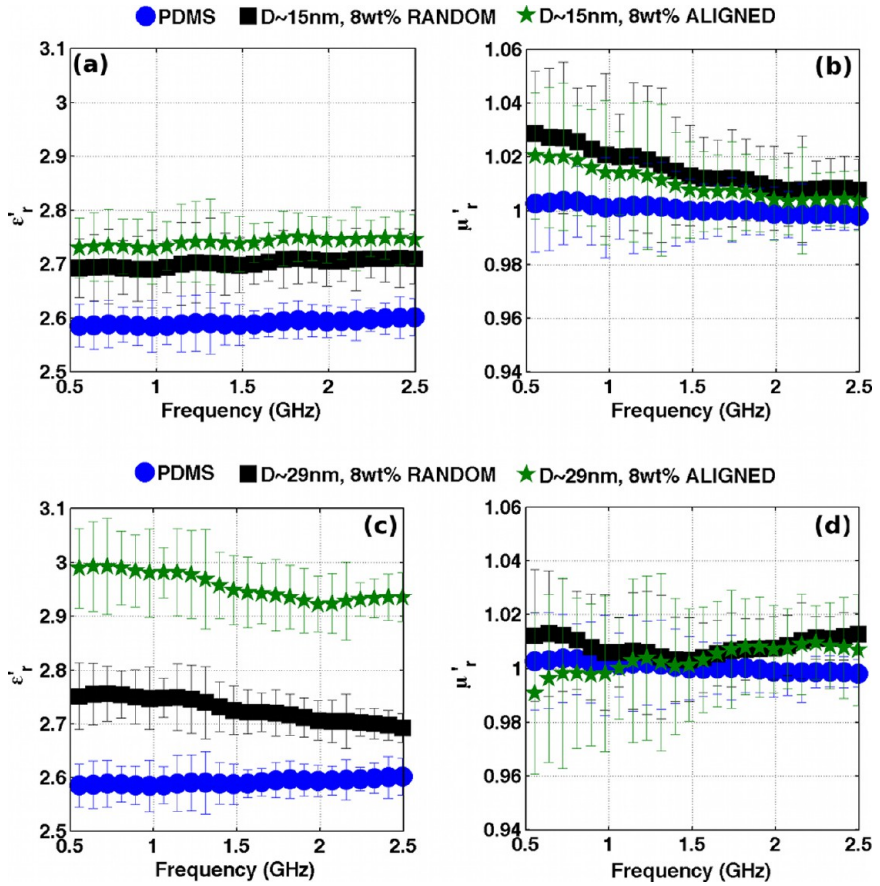

Figure 4. Radiofrequency characterization of aligned iron-oxide/PDMS PNCs. (a, c) Dielectric permittivity and (b, d) magnetic permeability obtained between 0.5 GHz and 2.5 GHz for pure PDMS (blue dots), random (black squares) and aligned (green stars) PNCs at ~8 wt % NPs concentration for (a, b) $D \approx 15$ nm and (c, d) $D \approx 29$ nm.

homogeneous filler distribution, the mold was thermally cured at 95 °C for 4 h, in absence of the magnetic field.

RESULTS AND DISCUSSION

Figure 2 shows a top-view (panels b and c) and a cross section (panels d and e), respectively, of the realized IONPs/PDMS aligned nanocomposites, both having a IONPs concentration of ~8 wt %. When exposed to magnetic field of direction parallel to the *z*-axis, IONPs organize in vertical domains aligned along *z*.[28−30] From a first comparison of images b and c in Figure 2, one can observe that aligned regions in the *x*-*y* plane are bigger for IONPs with diameter $D \approx 29$ nm. In order to quantify this difference, a statistical analysis based on the cumulative distribution of the areas covered by the aligned domains in the *x*-*y* plane was performed. Figure 2f displays the probability to obtain domain areas higher than a certain surface A, i.e., $P(a > A)$ for the two IONPs diameters investigated in this work (see the Supporting Information for further details on the computational method). In agreement with recent numerical computations,[29] we have found that the alignment is more efficient for bigger IONPs. Indeed, the curve obtained for $D \approx 15$ nm (red dots in Figure 2f) lies well below the one measured for $D \approx 29$ nm for $A > 200$ μm^2, and the probability to obtain domains of ~1000 μm^2 is almost 1 order of magnitude higher for $D \approx 29$ nm. On the other hand, smaller IONPs are prone to arrange into smaller agglomerates, because $P(a > A)$ for $D \approx 15$ nm is above the distribution obtained for $D \approx 29$ nm in the case of $A < 200$ μm^2.

The RF properties in the range 0.5−2.5 GHz of IONPs/PDMS PNCs were tested by means of a reflection/transmission method based on coplanar waveguides (CWG).[21] Briefly, an electromagnetic wave at a given frequency was guided in a section of bare CWG and let impact on a second CWG covered with the PNC under investigation. The implemented RF setup is sketched in Figure 3a and more details on the measurement procedure have been given in the Supporting Information and in ref 21. Reflected and transmitted signals in terms of scattering coefficients were measured and complex dielectric permittivity and magnetic permeability of the unknown sample ($\varepsilon_r = \varepsilon'_r - j\varepsilon''_r$ and $\mu_r = \mu'_r - j\mu''_r$) were computed following the methods reported in refs 21, 43, and 44.

The results of ε'_r and μ'_r RF measurements for pure PDMS matrix and PNC containing randomly dispersed IONPs with $D \approx 15$ nm at two different weight concentrations (2 and 8 wt %) are reported in Figure 3b, c. In agreement with existing literature,[45−47] frequency-dependent permittivity measurements on pure PDMS show an almost constant ε'_r, slightly lower than 2.6, and a real magnetic permittivity $\mu'_r \approx 1$. When IONPs are randomly dispersed into the PDMS matrix, ε'_r increases with IONPs concentration (squares and triangles in Figure 3b, c) and it reaches values as high as ~2.7 for 8 wt %, without relevant modifications of its dispersion behavior. A similar behavior has been observed also for IONPs of $D \approx 29$ nm (data for random 8 wt % sample are reported in Figure 4c, d). Concerning μ'_r, no significant deviations from unity (i.e., the value for pure PDMS) were observed for all the investigated

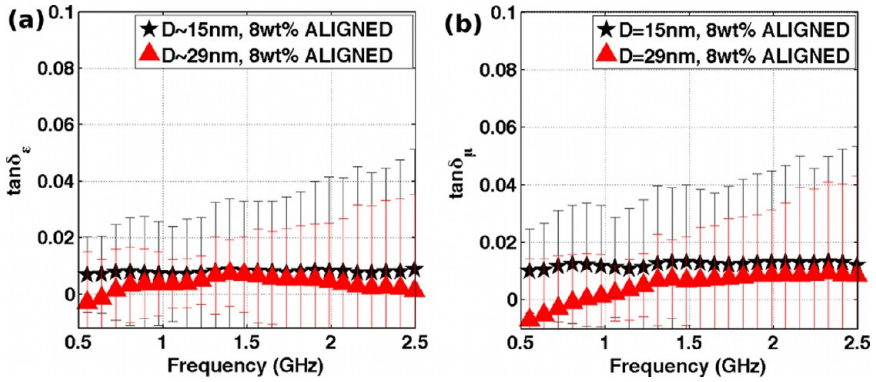

Figure 5. Dielectric and magnetic loss tangent of PNCs. Panel (a): Dielectric loss tangent for $D \approx 15$ nm (black stars) and $D \approx 29$ nm (red triangles). (b) Magnetic loss tangent for $D \approx 15$ nm (black stars) and $D \approx 29$ nm (red triangles).

weight percentages and IONPs diameters: even if a slight increase of the measured average value has been detected (Figure 3c), it lies well inside the measurement error bars obtained for pure PDMS. In the case of superparamagnetic fillers, this effect is usually assigned to the fact that the anisotropy energy of the PNC is not high enough to overcome the demagnetization arising from the thermal energy effects.[19] We should, however, notice that as mentioned above, the T_B of $D \approx 29$ nm is slightly above RT. Nevertheless, it seems that the anisotropy energy, which increases proportionally to IONPs volume, also in this case is not high enough to overcome the above-mentioned demagnetization, at least at the investigated concentrations. The very low hysteresis on the magnetization curve at 300 K for both IONPs diameters is a straightforward evidence of this fact and the unaltered behavior of magnetic permeability can be reasonably assigned to the superparamagnetic properties of IONPs, behaving thus as pure dielectric electromagnetic fillers.[19]

In aligned samples, we have instead found a remarkable difference between $D \approx 15$ nm and $D \approx 29$ nm. As mentioned above, these samples were prepared for the higher IONPs concentration (8 wt %), reassuring thus that the PDMS matrix is differentiated in the highest possible degree for this study. As shown in Figure 4, the higher the particles diameter, the more pronounced the alignment effect on ε'_r value. Indeed, when $D \approx 15$ nm, ε'_r values for random and aligned PNCs are almost comparable (Figure 4a). For $D \approx 29$ nm ε'_r is instead clearly higher for aligned NPs, approaching $\varepsilon'_r \approx 3$. This difference between aligned and not aligned samples suggests that ε'_r does not depend just on particles concentration and size distribution,[33,48,49] but also on their spatial alignment. Indeed, as already proved elsewhere, the presence of particle assemblies modifies the interactions at the interface between particles and the surrounding matrix affecting thus the ε'_r value.[31] It has been previously proved that IONPs with higher diameter ($D \approx 29$ nm) can be assembled in a more efficient way into the polymer matrix, leading to bigger clusters aligned in a wider volume.[29] As a consequence, the increased value of ε'_r obtained for bigger IONPs can be reasonably assigned to a better assembly of the clusters and their interaction compared to the smaller ones, because almost no differences have been recorded in ε'_r for random samples with different IONPs diameters. As for the case of samples with random dispersion, in samples with magnetically assembled IONPs, no variations of μ'_r where observed. Also in this case, this can be assigned to a thermal demagnetization process that, even in samples with wide aligned domains, does not allow a detectable modification of μ'_r.

The realized IONPs/PDMS PNCs have also been characterized in terms of dielectric and magnetic losses. For RF applications, and in particular for antennas' substrates, materials losses should be kept as low as possible in order to achieve high power efficiencies. As shown in Figure 5, average values of both tan $\delta_\varepsilon = \varepsilon''_r/\varepsilon'_r$ and tan $\delta_\mu = \mu''_r/\mu'_r$ are well below 0.02 up to 2.5 GHz, meaning that less than 2% of the electromagnetic energy passing through the PNCs is dissipated. This result let us envision that IONPs do not form conductive paths through the PNC and that, from the point of view of dielectric and magnetic loss, the PDMS matrix acts as an electrical insulator between the NPs and prevents them from conducting charges.[23]

CONCLUSION

In summary, we show that IONPs alignment into a polymeric matrix is an effective strategy to increase the dielectric permittivity of a PNC in the frequency range 0.5−2.5 GHz. Aligned chains of IONPs have been realized in PDMS host matrix by means of a magnetophoretic assembly method, based on the application of a static magnetic field during polymer curing. The effect on ε'_r is more pronounced for bigger particles, which align in wider-volume chains and lead to higher dielectric constants. Remarkably, magnetic and dielectric losses of the PNCs are kept below 0.02, letting us envision the suitability of the proposed material as substrate for RF applications.

ASSOCIATED CONTENT

Supporting Information

Synthesis of iron-oxide nanoparticles, magnetic characterization, measurement of the dielectric permittivity and magnetic permeability, and cluster size probability estimation. This material is available free of charge via the Internet at http://pubs.acs.org.

AUTHOR INFORMATION

Corresponding Author

*E-mail: ferruccio.pisanello@iit.it. Tel: +39 08321816232. Fax: +39 08321816208.

Author Contributions

The manuscript was written through contributions of all authors. All authors have given approval to the final version of the manuscript.

Notes

The authors declare no competing financial interest.

■ ACKNOWLEDGMENTS

This work was financially supported by the Italian PON project "ITEM", the FP7 starting ERC Grant NANOARCH Contract 240111) and the Italian FIRB grant (contract #RBAP115AYN).

■ REFERENCES

(1) Kumar, S. K.; Krishnamoorti, R., Nanocomposites: Structure, Phase Behavior, and Properties. In *Annual Reviews of Biomedical Engineering*; Prausnitz, J. M., Doherty, M. F., Segalman, M. A., Eds.; Annual Reviews: Palo Alto, CA, 2010; Vol. *1*, pp 37−58.
(2) Rafiee, M. A.; Rafiee, J.; Srivastava, I.; Wang, Z.; Song, H.; Yu, Z. Z.; Koratkar, N. *Small* **2009**, *6*, 179−183.
(3) Pushparaj, V. L.; Shaijumon, M. M.; Kumar, A.; Murugesan, S.; Ci, L.; Vajtai, R.; Linhardt, R. J.; Nalamasu, O.; Ajayan, P. M. *Proc. Natl. Acad. Sci. U.S.A.* **2007**, *104*, 13574−13577.
(4) Hu, N.; Karube, Y.; Yan, C.; Masuda, Z.; Fukunaga, H. *Acta Mater.* **2008**, *56*, 2929−2936.
(5) Kang, I.; Schulz, M. J.; Kim, J. H.; Shanov, V.; Shi, D. *Smart Mater. Struct.* **2006**, *15*, 737.
(6) Kashiwagi, T.; Grulke, E.; Hilding, J.; Groth, K.; Harris, R.; Butler, K.; Shields, J.; Kharchenko, S.; Douglas, J. *Polymer* **2004**, *45*, 4227−4239.
(7) Martiradonna, L.; Carbone, L.; Tandaechanurat, A.; Kitamura, M.; Iwamoto, S.; Manna, L.; De Vittorio, M.; Cingolani, R.; Arakawa, Y. *Nano Lett.* **2008**, *8*, 260−264.
(8) Qualtieri, A.; Martiradonna, L.; Stomeo, T.; Todaro, M. T.; Cingolani, R.; Vittorio, M. D. *Microelectron. Eng.* **2009**, *86*, 1127−1130.
(9) Liu, J. R.; Itoh, M.; Machida, K. *Appl. Phys. Lett.* **2006**, *88*, 062503−062503.
(10) Chen, Y.; Gao, P.; Zhu, C.; Wang, R.; Wang, L.; Cao, M.; Fang, X. *J. Appl. Phys.* **2009**, *106*, 54303.
(11) Hussain, S.; Youngs, I. J.; Ford, I. J. *J. Phys. D: Appl. Phys.* **2007**, *40*, 5331.
(12) Chiu, S. C.; Yu, H. C.; Li, Y. Y. *J. Phys. Chem. C* **2010**, *114*, 1947−1952.
(13) Jia, K.; Zhao, R.; Zhong, J.; Liu, X. *J. Magn. Magn. Mater.* **2010**, *322*, 2167−2171.
(14) Liu, J. R.; Itoh, M.; Machida, K. *Appl. Phys. Lett.* **2003**, *83*, 4017−4019.
(15) Kraus, J. D.; Marhefka, R. J., *Antenna for All Applications*; McGraw-Hill: New York, 2002.
(16) Matsumoto, M.; Miyata, Y. *IEEE Trans. Magn.* **1997**, *33*, 4459−4464.
(17) Baibarac, M.; Gomez-Romero, P. *J. Nanosci. Nanotechnol.* **2006**, *6*, 289−302.
(18) Abbas, S. M.; Dixit, A. K.; Chatterjee, R.; Goel, T. C. *J. Magn. Magn. Mater.* **2007**, *309*, 20−24.
(19) Yang, T. I.; Brown, R. N. C.; Kempel, L. C.; Kofinas, P. *J. Magn. Magn. Mater.* **2008**, *320*, 2714−2720.
(20) Kong, J.; Liu, J.; Wang, F.; Luan, L.; Itoh, M.; Machida, K. *Appl. Phys. A: Mater. Sci. Process.* **2011**, *105*, 351−354.
(21) Pisanello, F.; De Paolis, R.; Lorenzo, D.; Nitti, S.; Monti, G.; Fragouli, D.; Athanassiou, A.; Manna, L.; Tarricone, L.; De Vittorio, M.; Martiradonna, L. *Microelectron. Eng.* **2012**, in press http://dx.doi.org/10.1016/j.mee.2012.11.013.
(22) Yang, T. I.; Brown, R. N. C.; Kempel, L. C.; Kofinas, P. *J. Nanopart. Res.* **2010**, *12*, 2967−2978.
(23) Yang, T.; Brown, R.; Kempel, L.; Kofinas, P. *Nanotechnology* **2011**, *22*, 105601.
(24) Liu, X.; Geng, D.; Shang, P.; Meng, H.; Yang, F.; Li, B.; Kang, D.; Zhang, Z. *J. Phys. D: Appl. Phys.* **2008**, *41*, 175006.
(25) Feng, H.; Zhuo, R.; Chen, J.; Yan, D.; Feng, J.; Li, H.; Cheng, S.; Wu, Z.; Wang, J.; Yan, P. *Nanoscale Res. Lett.* **2009**, *4*, 1452−1457.
(26) Chikazumi, S.; Taketomi, S.; Ukita, M.; Mizukami, M.; Miyajima, H.; Setogawa, M.; Kurihara, Y. *J. Magn. Magn. Mater.* **1987**, *65*, 245−251.
(27) Wang, H.; Chen, Q. W.; Sun, L. X.; Qi, H.; Yang, X.; Zhou, S.; Xiong, J. *Langmuir* **2009**, *25*, 7135−7139.
(28) Fragouli, D.; Buonsanti, R.; Bertoni, G.; Sangregorio, C.; Innocenti, C.; Falqui, A.; Gatteschi, D.; Cozzoli, P. D.; Athanassiou, A.; Cingolani, R. *ACS Nano* **2010**, *4*, 1873−1878.
(29) Bertoni, G.; Torre, B.; Falqui, A.; Fragouli, D.; Athanassiou, A.; Cingolani, R. *J. Phys. Chem. C* **2011**, *115*, 7249−7254.
(30) Lorenzo, D.; Fragouli, D.; Bertoni, G.; Innocenti, C.; Anyfantis, G. C.; Davide Cozzoli, P.; Cingolani, R.; Athanassiou, A. *J. Appl. Phys.* **2012**, *112*, 083927−083927−8.
(31) Kim, K. H.; Yamaguchi, M.; Orikasa, H.; Kyotani, T. *Solid State Commun.* **2006**, *140*, 491−494.
(32) Goubault, C.; Leal-Calderon, F.; Viovy, J. L.; Bibette, J. *Langmuir* **2005**, *21*, 3725−3729.
(33) Hallouet, B.; Wetzel, B.; Pelster, R. *J. Nanomater.* **2007**, *2007*, 34527.
(34) Rogers, J. A.; Someya, T.; Huang, Y. *Science* **2010**, *327*, 1603−1607.
(35) Khodasevych, I. E.; Shah, C. M.; Sriram, S.; Bhaskaran, M.; Withayachumnanku, W.; Ung, B. S. Y.; Lin, H.; Rowe, W. S. T.; Abbott, D.; Mitchell, A. *Appl. Phys. Lett.* **2012**, *100*, 061101.
(36) Pisanello, F.; Martiradonna, L.; Sileo, L.; Brunetti, V.; Vecchio, G.; Malvindi, M. A.; Morello, G.; Zanella, M.; Pompa, P. P.; Manna, L.; De Vittorio, M.; *Microelectron. Eng.* **2012**, in press http://dx.doi.org/10.1016/j.mee.2013.02.019
(37) Shah, C. M.; Sriram, S.; Bhaskaran, M.; Nasabi, M.; Nguyen, T. G.; Rowe, W. S. T.; Mitchell, A. *J. Microelectromech. Syst.* **2012**, *21*, 1410−1416.
(38) William, W. Y.; Falkner, J. C.; Yavuz, C. T.; Colvin, V. L. *Chem. Commun.* **2004**, 2306−2307.
(39) Hou, Y.; Xu, Z.; Sun, S. *Angew. Chem., Int. Ed.* **2007**, *119*, 6445−6448.
(40) Bodnarchuk, M. I.; Kovalenko, M. V.; Groiss, H.; Resel, R.; Reissner, M.; Hesser, G.; Lechner, R. T.; Steiner, W.; Schäffler, F.; Heiss, W. *Small* **2009**, *5*, 2247−2252.
(41) Watarai, H.; Suwa, M.; Iiguni, Y. *Anal. Bioanal. Chem.* **2004**, *378*, 1693−1699.
(42) Das, S.; Ranjan, P.; Maiti, P. S.; Singh, G.; Leitus, G.; Klajn, R. *Adv. Mater.* **2013**, *25*, 422−426.
(43) Barry, W. *IEEE Trans. Microwave Theory* **1986**, *34*, 80−84.
(44) Kang, B.; Cho, J.; Cheon, C.; Kwon, Y. *IEEE Microwave Wireless Compon.* **2005**, *15*, 381−383.
(45) Molberg, M.; Leterrier, Y.; Plummer, C. J. G.; Walder, C.; Lowe, C.; Opris, D. M.; Nuesch, F. A.; Bauer, S.; Manson, J. A. E. *J. Appl. Phys.* **2009**, *106*, 054112.
(46) Koulouridis, S.; Kiziltas, G.; Zhou, Y.; Hansford, D. J.; Volakis, J. L. *IEEE Trans. Microwave Theory* **2006**, *54*, 4202−4208.
(47) *MIT Materials Properties,* http://www.mit.edu/~6.777/matprops/pdms.htm.
(48) Fu, L.; Macedo, P. B.; Resca, L. *Phys. Rev. B: Condens. Matter Mater. Phys.* **1993**, *47*, 13818.
(49) Spanoudaki, A.; Pelster, R. *Phys. Rev. B: Condens. Matter Mater. Phys.* **2001**, *64*, 064205.